Brain structure reflects empathy and psychopathy in incarcerated males

Marcin A. Radecki[a,b,*], Erika Sampaolo[a], Giada Lettieri[a,c], Giacomo Handjaras[a], Carla L. Harenski[d], Sara Palumbo[e], Silvia Pellegrini[e], Pietro Pietrini[f,*], Kent A. Kiehl[d,g,†], & Luca Cecchetti[a,†]

[a] Social and Affective Neuroscience Group, IMT School for Advanced Studies Lucca, Lucca, Italy

[b] Autism Research Centre, Department of Psychiatry, University of Cambridge, Cambridge, UK

[c] Crossmodal Perception and Plasticity Laboratory, Institute of Research in Psychology and Institute of Neuroscience, Université Catholique de Louvain, Louvain-la-Neuve, Belgium

[d] Mind Research Network and Lovelace Biomedical and Environmental Research Institute, Albuquerque, NM, USA

[e] Department of Clinical and Experimental Medicine, University of Pisa, Pisa, Italy

[f] Molecular Mind Laboratory, IMT School for Advanced Studies Lucca, Lucca, Italy

[g] Departments of Psychology, Neuroscience, and Law, University of New Mexico, Albuquerque, NM, USA

[†] denotes equal senior authorship

* denotes corresponding authors: Marcin A. Radecki (mr945@medschl.cam.ac.uk) and Pietro Pietrini (pietro.pietrini@imtlucca.it), IMT School for Advanced Studies Lucca, Piazza San Francesco 19, 55100 Lucca, Italy

Running title: Empathy, psychopathy, and brain structure

Word count

Abstract: 244

Introduction: 1,043

Materials and Methods: 1,315

Results: 1,007

Discussion: 1,610

Conclusions: 115

Main text: 5,090

27.05.2023

Abstract

Whether brain structure could reflect empathy and psychopathy in the same antisocial population is unknown. In White adult males from prison (N = 549, M_{age} = 34 ± 11 years), we measured empathy with the Perspective Taking (IRI-PT) and Empathic Concern (IRI-EC) subscales of the Interpersonal Reactivity Index, and psychopathic traits with the Psychopathy Checklist–Revised or Youth Version (PCL-R/YV). A subsample (N = 278, M_{age} = 36 ± 11 years) underwent MRI, from which we derived cortical thickness (CT) and surface area (SA). CT did not relate to IRI-PT or IRI-EC, while SA of the left inferior temporal gyrus (L ITG) related negatively to IRI-PT and positively to PCL-R and PCL-R item 8 (Callousness/Lack of Empathy). L-ITG SA predicted scores on IRI-PT – but not IRI-EC – in an out-of-sample test (R^2 = 0.030). Mapping onto the histological BigBrain gradient, higher scores on IRI-PT – but not IRI-EC – entailed a progressive SA reduction from Bin 1 (sensorimotor) to Bin 5 (limbic). Psychopaths (PCL-R/YV ≥ 30, N = 73/39) had: (1) reduced IRI-PT and IRI-EC scores (Cohen's Ds = -0.423, -0.564, respectively); (2) increased L-ITG SA (Cohen's D = 0.560); (3) increased global SA (Cohen's D = 0.480); and (4) reduced SA covariance between the left precentral and left isthmus-cingulate cortices. There were no group differences in global, modular, or nodal SA covariance, as indexed by canonical graph-theoretical metrics. We provide novel insights into the brain correlates of empathy and psychopathy in incarcerated males.

Keywords: Empathy; Psychopathy; Brain structure; Machine learning; Structural covariance

Introduction

The landscape of self-report measures of empathy is vast (de Lima & de Lima Osório, 2021), with one of the most popular ones being the Interpersonal Reactivity Index (IRI; Davis, 1980). Its Perspective Taking (IRI-PT) and Empathic Concern (IRI-EC) subscales are often used to denote cognitive and affective empathy, respectively (Jolliffe & Farrington, 2004; Vachon et al., 2014; van Langen et al., 2014). IRI-PT was defined to measure the "tendency to spontaneously adopt the psychological point of view of others" while IRI-EC the "feelings of sympathy and concern for unfortunate others" (Davis, 1983, pp. 113–114). The mirror opposite of empathy could be the callousness observed in psychopathy, a personality condition generally characterized by pervasive antisocial behavior (De Brito et al., 2021a) and most commonly assessed with the Psychopathy Checklist–Revised (PCL-R; Hare, 1991; 2003; Sanz-García et al., 2021). Here, we aim to better understand empathy and psychopathy, as defined above, by examining brain structure in incarcerated males.

A negative relationship between empathy and antisocial phenotypes, including psychopathy, is supported by at least 12 meta-analyses (Miller & Eisenberg, 1988; Jolliffe & Farrington, 2004; Marsh & Blair, 2008; Wilson et al., 2011; Dawel et al., 2012; Vachon et al., 2014; van Langen et al., 2014; Morrow, 2019; Blötner et al., 2021; Burghart & Mier, 2022; Campos et al., 2022; Johnson et al., 2022). Across antisocial populations, cognitive empathy is reduced/impaired to a greater extent than affective empathy (Jolliffe & Farrington, 2004; Vachon et al., 2014; van Langen et al., 2014; Morrow, 2019; Campos et al., 2022), whereas psychopathy relates more negatively to affective empathy (Burghart & Mier, 2022; Campos et al., 2022). Psychopaths also score lower on self-report questionnaires but not necessarily performance tests of cognitive empathy (Campos et al., 2022; but see also Wilson et al., 2011; Dawel et al., 2012), which would stand in line with evidence from antisocial-personality individuals (Johnson et al., 2022). This may indicate psychopathic deficits in empathic tendency rather than ability (Keysers & Gazzola, 2014; Drayton et al., 2018). Looking at the brain structure of incarcerated males, who are 13 times more likely to meet the psychopathy criteria compared to the general population (prevalence: 15.7% vs 1.2%, respectively; Sanz-García et al., 2021), may prove helpful in explaining this reduced tendency and/or impaired ability to empathize.

The brain correlates of empathy have been explored in a number of functional meta-analyses, with at least 14 on cognitive empathy (Spreng et al., 2009; Van Overwalle, 2009; Van Overwalle & Baetens, 2009; Mar, 2011; Sperduti et al., 2011; Bzdok et al., 2012; Schurz et al., 2013; Andrews-Hanna et al., 2014; Schurz et al., 2014; van Veluw & Chance, 2014; Molenberghs et al., 2016; Arioli et al., 2021; Diveica et al., 2021; Schurz et al., 2021) and 10 on affective empathy (Fan et al., 2011; Lamm et al., 2011; Bzdok et al., 2012; Timmers et al., 2018; Jauniaux et al., 2019; Xiong et al., 2019; Fallon et al., 2020; Arioli et al., 2021; Diveica et al., 2021; Schurz et al., 2021). Cognitive empathy most consistently relates to the medial prefrontal cortex (especially its dorsal portions), temporo-parietal junction, precuneus, and temporal gyri. Affective empathy most consistently relates to the insula (especially its anterior portions) and cingulate cortex (especially its anterior and middle portions). A 2021 meta-analysis (Schurz et al., 2021) showed that the brain-activation clusters underlying empathy can be positioned along a principal gradient of macroscale cortical organization, with cognitive empathy tilting toward the abstract/transmodal end (largely mapping onto the default-mode network; Margulies et al., 2016; Huntenburg et al., 2018) and affective empathy toward the sensory/unimodal end. With no structural meta-analyses on the topic, there is a need for a better understanding of how brain structure reflects empathy (for study examples, see Banissy et al., 2012; Eres et al., 2015; Valk et al., 2017).

The brain correlates of antisocial phenotypes, including psychopathy, were explored in at least four structural meta-analyses (Yang & Raine, 2009; Aoki et al., 2014; Rogers & De Brito, 2016; De Brito et al., 2021b). They found both “cognitive-empathy” brain regions (e.g., medial prefrontal cortex) and “affective-empathy” brain regions (e.g., insula) to be generally reduced in gray-matter volume among antisocial populations. These findings are corroborated by more recent large-sample studies (N > 600) on gray-matter differences in incarcerated homicide offenders (Sajous-Turner et al., 2020) or cortical-thickness (CT) and surface-area (SA) differences in community-dwelling antisocial individuals (Carlisi et al., 2020). A structural review of 11 studies in psychopathy and 21 studies in the general population (Korponay & Koenigs, 2021) suggested that the relationship between a psychological variable (here, impulsiveness) and brain structure (here, gray-matter volume) may vary by psychopathy status (for broader reviews, see Johanson et al., 2020; Jalava et al., 2021). This psychopathic “difference by kind rather than degree” may also pertain to cognitive empathy, operationalized as emotion recognition (Pera-Guardiola et al., 2016). A similar

picture emerges from the functional literature, where “empathic” brain regions also distinguish antisocial populations (Yang & Raine, 2009; Poeppl et al., 2019; Deming & Koenigs, 2020; Dugré & Potvin, 2021). As some brain regions play a role in both empathy and antisocial behavior, could their atypical structure or structural covariance account for reductions/impairments in empathy? Exploring the antisocial brain may further prove helpful in understanding psychopathic traits beyond callousness, such as impulsiveness or any of the other 18 traits (De Brito et al., 2021a).

In at least 278 White adult males from prison, we tested whether: (1) brain structure (i.e., MRI-derived CT and SA) relates to empathy; (2) identified brain structure relates to psychopathic traits; (3) identified brain structure and empathy differ by psychopathy status; (4) empathy can be predicted from brain structure using machine learning; (5) empathy follows a gradient of microstructural organization; (6) global brain structure differs by psychopathy status; (7) structural covariance – global, modular, and nodal – differs by psychopathy status. While machine learning has been utilized to predict psychopathic traits from brain structure in a prison population (Steele et al., 2017), prediction of empathy in this context remains untapped, and structural covariance in psychopathy may have been evaluated only once and using CT (Yang et al., 2012). We add to a growing neuroimaging literature on social-affective phenotypes in incarcerated males (e.g., Harenski et al., 2018; Caldwell et al., 2019; Deming et al., 2020).

Materials and Methods

Participants

The participants were White adult males from New Mexico and Wisconsin prisons – the racial composition was kept homogeneous due to planned genetic analyses (not conducted here). As shown in *Table 1*, they represented the behavioral sample (N = 549) and the brain-structural (sub)sample (N = 278). In the behavioral sample, the participants provided data on empathy and psychopathy, among others; in the brain-structural sample, they also provided a usable MRI scan (for the characteristics of further subsamples with additional data, see *Table S1*). The participants committed one of three types of crime: (1) non-violent or minimally violent; (2) non-homicide violent; or (3) homicide (for an exhaustive description of the inclusion criteria, see Sajous-Turner et al., 2020). In compliance with the Declaration of Helsinki, the participants provided informed consent and the research protocol was approved by the IRB of the University of New Mexico (and Ethical and Independent Review Services for data collection post June 2015).

Table 1 | Participant characteristics

Sample		**Behavioral**	**Brain-structural**
N		549	278
Sex			
	Male	549	278
Race			
	White	549	278
Ethnicity			
	Non-Hispanic	335	208
Handedness			
	Right-handed	454	230
Age [years]			
	Mean ± SD	34.004 ± 10.867	36.155 ± 10.500
	Median	33	35
	Range	18-70	18-65
WAIS-III [IQ]			
	Mean ± SD	97.996 ± 14.238	100.097 ± 14.638
	Median	97	100
	Range	63-137	66-131
Crime type			
	Non-violent/min. violent	81	41

Non-homicide violent	365	176
Homicide	103	61
PCL-R/YV		
Mean ± SD	20.843 ± 6.871	20.701 ± 7.010
Median	21	21.100
Range	3-37.600	3-37
*PCL version**		
PCL-R	498	278

Note. WAIS-III = Vocabulary and Matrix Reasoning subtests of the Wechsler Adult Intelligence Scale, third ed; PCL-R/YV = Psychopathy Checklist–Revised/Youth Version; * The Youth Version was administered to 48 18-year-olds and three 19-year-olds in the behavioral sample. The brain-structural sample is a subsample of the behavioral sample.

MRI

In 325 participants, we acquired high-resolution T1-weighted MRI scans on the Mind Research Network Siemens MAGNETOM Avanto 1.5-T mobile scanner, stationed at one of the prisons. We used a 12-channel MPRAGE pulse sequence, kindly provided by the Massachusetts General Hospital Radiology Department. The scanning parameters were as follows: repetition time = 2,530 ms; echo times = 1.64 ms, 3.50 ms, 5.36 ms, 7.22 ms; inversion time = 1100 ms; flip angle = 7°; slice thickness = 1.3 mm; matrix size = 256 × 256. The sequence yielded 128 sagittal slices with an in-plane resolution of 1.0 mm × 1.0 mm^2.

To preprocess the data, we adapted some of the major steps from the Human Connectome Project pipeline (Glasser et al., 2013). T1-weighted images were: (1) reoriented with *fslreorient2std* in FSL 5.0.9 (Jenkinson et al., 2012); (2) aligned to the ACPC plane with: *robustfov*, *convert_xfm*, *flirt*, *aff2rigid*, and *applywarp* in FSL 5.0.9; and, finally, (3) skull-stripped and parcellated according to the Desikan-Killiany atlas (Desikan et al., 2006) with *recon-all* in FreeSurfer 6.0.0 (Fischl, 2012). The output data were rejected in case of *recon-all* errors or major failures in white/gray-matter segmentation, surface delineation, and/or

regional parcellation, as confirmed by visual inspection in FreeView 2.0. This quality check passed data for 278 participants. In analysis, we included CT and SA rather than cortical volume for improved specificity (Rimol et al., 2012). To denote brain size, we used total intracranial volume (TIV).

Empathy

We measured cognitive and affective empathy, respectively, using the IRI-PT and IRI-EC subscales of IRI (which also includes the Fantasy and Personal Distress subscales; Davis, 1980). Each subscale includes seven items scored on a five-point scale ranging from "Does not describe me well" (0 points) to "Describes me very well" (4 points) (*Table S2*). Possible scores thus range 0-28 points for each subscale, with higher scores indicating higher empathy.

Psychopathy

We measured psychopathic traits using PCL-R (Hare, 1991; 2003) or its Youth Version (PCL:YV; Forth et al., 2003) (*Table 1*). PCL-R/YV is an expert-rated semi-structured interview that evaluates 20 traits, saturating two Factors or four Facets (*Table S3*), scored on a three-point scale with 0, 1, and 2 points, indicating no evidence, some evidence, and pervasive evidence, respectively. The total score is a sum of the 20 items, thus ranging 0-40 points, with higher scores indicating higher psychopathic traits and a recommended "diagnostic" cut-off at 30 points (Hare, 1991; 2003). For items omitted due to insufficient information, we used a prorating formula, yielding decimal scores. Complete Facet-level data were available for 525 (out of 549) and 268 (out of 278) participants.

Following both behavioral (e.g., Blair et al., 2004) and neuroimaging (e.g., Fede et al., 2016) work in incarcerated males, we identified psychopaths at ≥ 30 and non-psychopaths at < 20 points on PCL-R/YV. In a subsample that was administered the Structured Clinical Interview for DSM-IV (SCID; First & Gibbon, 2004), 77% of psychopaths met the antisocial-personality criteria, whereas 49% of antisocial-personality individuals met the psychopathy criteria (*Table S4*). This is largely in line with the literature, where ~80-90% of psychopaths are estimated to meet the antisocial-personality criteria, and ~25-40% of antisocial-personality individuals are estimated to meet the psychopathy criteria (De Brito et al., 2021a). In *Table 2*, we characterize psychopaths and non-psychopaths in the two samples.

Table 2 | Psychopaths' and non-psychopaths' characteristics

Sample	**Behavioral**			**Brain-structural**		
	Psychopaths	*Non-psychopaths*	Difference	*Psychopaths*	*Non-psychopaths*	Difference
N	73	222		39	114	
Ethnicity			0.570			0.634
Non-Hispanic	45	145		29	89	
Handedness			0.027			0.064
Right-handed	53	187		28	97	
Age [years]			0.021			0.140
Mean ± SD	32.151 ± 10.140	35.824 ± 11.223		34.513 ± 8.720	37.439 ± 10.583	
Median	31	35		33	37	
Range	18-54	18-70		20-53	18-65	
WAIS-III [IQ]			0.053			0.230
Mean ± SD	101.452 ± 14.815	97.608 ± 14.688		103.359 ± 12.936	100.114 ± 16.008	
Median	100	97		103	100	

Range	72-137	66-134		79-131	66-128	
Crime type			0.432			0.466
Non-violent/min. violent	9	34		5	21	
Non-homicide violent	46	148		22	68	
Homicide	18	40		12	25	
TIV [mm^3]			–			0.322
Mean ± SD	–	–		1.687e+06 ± 1.128e+05	1.663e+06 ± 1.367e+05	
BSV [mm^3]			–			0.163
Mean ± SD	–	–		1.200e+06 ± 8.349e+04	1.175e+06 ± 1.039e+05	
PCL-R/YV			–			–
Mean ± SD	31.748 ± 1.903	14.122 ± 3.790		31.287 ± 1.438	13.786 ± 3.882	
Median	31	15		31	14.550	
Range	30-37.600	3-19		30-37	3-19	
PCL version			0.013			–

PCL-R	62	209	39	114

Note. WAIS-III = Vocabulary and Matrix Reasoning subtests of the Wechsler Adult Intelligence Scale, third ed.; IQ = intelligence quotient, converted from the WAIS-III; TIV = total intracranial volume; BSV = brain segmentation volume including cerebellum but excluding ventricles, cerebrospinal fluid, and dura; PCL-R/YV = Psychopathy Checklist–Revised/Youth Version. Difference was measured with Wilcoxon's rank-sum test for continuous variables and χ^2 test for categorical ones; reported are P-values.

Intelligence

We measured verbal and performance intelligence using the Vocabulary and Matrix Reasoning subtests, respectively, of the Wechsler Adult Intelligence Scale, third ed. (WAIS-III; Wechsler, 1997). Vocabulary score ranges 0-66 points and Matrix Reasoning score 0-26 points, with higher scores indicating higher intelligence. We summed the two scores and converted them into an IQ estimate.

Impulsivity

In 212 participants in the brain-structural sample, we additionally measured impulsivity using the Barratt Impulsiveness Scale (BIS-11; Patton et al., 1995). The total score ranges 30-120 points, with higher scores indicating higher impulsivity. See *Table S1*.

Prison time and psychiatric disorders

In 257 participants in the behavioral sample, we additionally recorded prison time and psychiatric disorders. Prison time was estimated in months using institutional movement records or self-reports from PCL-R/YV interviews. It was further divided by age and square-root-transformed to address skewness. To determine DSM-IV Axis-I and Axis-II disorders, we used SCID (First & Gibbon, 2004). See *Table S1* and *Table S4*.

Statistical analysis

We ran statistical analysis in MATLAB R2020b (MathWorks Inc., Natick, MA, USA) and shared the code on OSF at https://osf.io/xazf6/?view_only=b9652ff8801b489a9520ad7b165d592a.

First, we tested whether IRI-PT/IRI-EC scores can be explained with CT/SA. As in all subsequent analyses reported in *Results* – controlling at least for age, WAIS-III, and crime type, and additionally for PCL version or TIV – effects with significant P-values ($P < 0.05$) were permuted by randomly shuffling the values of the independent variable of interest (here, brain region) and finally dividing the rank of the observed value (here, T-value) by the number of permutations plus 1 (here, $N_p = 100{,}000$ and for the graph-theoretical analysis, $N_p = 25{,}000$; divided by 2 when a two-tailed distribution). P-values were then corrected for multiple testing using Bonferroni's method (Bland & Altman, 1995) across the number of tests (here, for the

68 Desikan-Killiany brain regions) at $P_{Bon} < 0.05$. We fitted four robust linear regressions across the cortex as follows:

IRI-PT/IRI-EC ~ CT/SA + age + WAIS-III + crime type + TIV

Secondly, we tested whether identified brain regions explained PCL-R or PCL-R item 8 (Callousness/Lack of Empathy) scores. Thirdly, we tested whether identified brain regions and IRI scores differed by psychopathy status, using Cohen's D on covariate-corrected data to quantify effect size (for the formula, see *Section S1*). Fourthly, we tested whether identified brain regions explained PCL-R Factor/Facet scores, and whether the brain-related IRI score also related to PCL-R and PCL-R item 8 scores. Fifthly, we used machine learning to predict IRI scores from covariate-corrected brain data: LASSO regression with K-fold cross-validation and permutation-based significance testing for mean squared error (MSE) (for the formulae, see *Section S1*). Sixthly, we tested the interaction effect between IRI scores and the BigBrain bins on covariate-corrected brain data. These bins represent a sensory-fugal gradient of structural covariance (Paquola et al., 2019; 2021), which is based on the histological BigBrain model (Amunts et al., 2013) and translates to the Desikan-Killiany atlas (Larivière et al., 2021). We additionally divided participants into four groups based on the mean and standard deviation, and used the following mixed-effects formula on covariate-corrected data:

Corrected CT/SA ~ IRI score/group * BigBrain bin + (1 | participant)

Seventhly, we tested global brain structure by psychopathy status. Finally, we tested structural covariance by psychopathy status using non-parametric combination (Winkler et al., 2016), permutation-based significance testing, and family-wise-error (FWE) correction (Nichols & Holmes, 2001) for global and edge-wise covariance as well as six conventional graph-theoretical metrics: modularity, global efficiency, local efficiency, strength, degree, and betweenness centrality (Rubinov & Sporns, 2010) (*Section S2*). For brain visualizations, we used the ENIGMA Toolbox (Larivière et al., 2021) and Surf Ice (https://www.nitrc.org/projects/surfice/; for our centroid MNI coordinates, see *Table S5*).

Results

Empathy, psychopathy, and brain structure

When explaining IRI-PT with CT, we found no significant brain region (Ps ≥ 0.069; *Figure S1*). When explaining IRI-PT with SA, we found that L ITG had a negative effect on IRI-PT, β = -0.003 [95% CI: -0.005, -0.001], P_{Bon} = 0.037, adj. R^2 = 0.101, N = 278 (*Figure 1*). When explaining IRI-EC with CT and SA, we found no significant brain region (Ps_{Bon} = 1, P_{Bon} ≥ 0.196, respectively; *Figure S1*). As CT did not relate to either IRI subscale, we ran all subsequent analyses on SA only. For sensitivity analyses testing L-ITG SA, see *Sections S3* and *S4*.

We further took L ITG as a region of interest (ROI) to find that its SA had a positive effect on PCL-R, β = 0.003 [95% CI: 5.000e-04, 0.006], P_{Bon} = 0.031, adj. R^2 = 0.035, and a non-self-report measure of empathy, PCL-R item 8 (Callousness/Lack of Empathy), β = 3.321e-04 [95% CI: 1.000e-04, 6.000e-04], P_{Bon} = 0.033, adj. R^2 = 0.032, N = 275 (*Figure 1*).

Drawing from the brain-structural sample, we found that psychopaths (N = 39) had increased L-ITG SA compared to non-psychopaths (N = 114), β = 172.472 [95% CI: 46.547, 298.397], P_p = 0.009, adj. R^2 = 0.432, Cohen's D = 0.560 (*Figure 1*). Drawing from the behavioral sample, we found that psychopaths (N = 73) scored lower than non-psychopaths (N = 222) on both IRI-PT, β = -2.185 [95% CI: -3.587, -0.783], P_{Bon} = 0.005, adj. R^2 = 0.084, Cohen's D = -0.423, and IRI-EC, β = -2.523 [95% CI: -3.898, -1.148], P_{Bon} = 0.001, R^2 = 0.103, Cohen's D = -0.564 (*Figure 1*). For analysis of PCL-R/YV Factors and Facets, see *Section S5*.

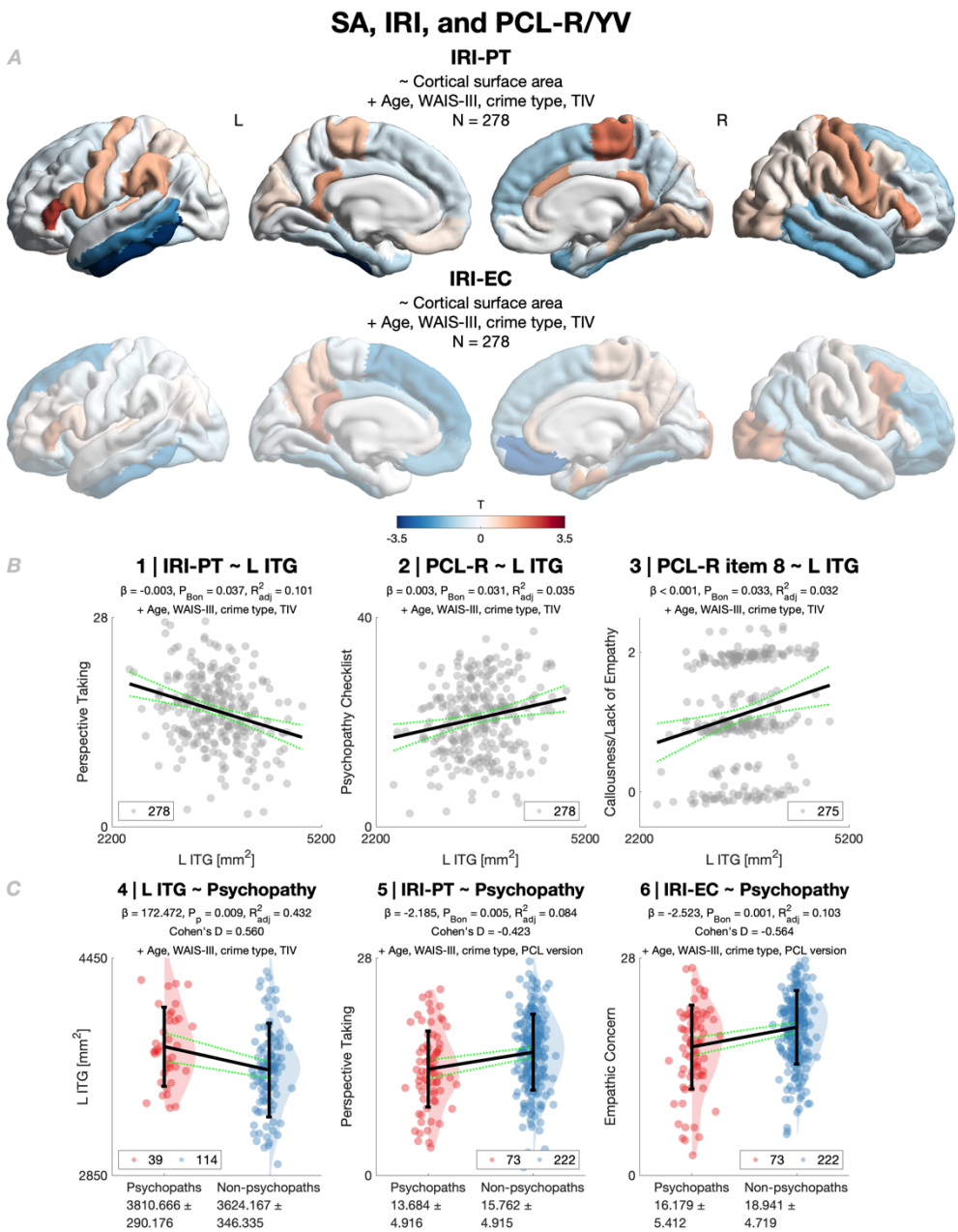

Figure 1 | SA, IRI, and PCL-R/YV. Panel A shows T-value maps for regional SA explaining IRI-PT and IRI-EC. L ITG survived the Bonferroni correction for IRI-PT, while no brain region survived the correction for IRI-EC. Panel B shows a negative effect of L-ITG SA on IRI-PT and its positive effect on PCL-R and PCL-R item 8 (Callousness/Lack of Empathy) following permutation. Panel C shows increased L-ITG SA and reduced IRI-PT and IRI-EC scores in psychopaths following permutation. All models include 95% confidence bounds in dotted green. Models 4-6 include a kernel-density estimation for each group, with error bars representing standard deviation. All models controlled for the covariates outlined after the plus sign. For an opaque T-value map for IRI-EC, see *Figure S1*.

Machine learning of empathy from brain structure

Next, we investigated whether IRI scores could be predicted from covariate-corrected SA using machine learning. We randomly assigned 80% of the participants (N = 223) into the training set and the remaining 20% (N = 55) into the test set, stratifying by IRI-PT (i.e., approximately equating between the training and test sets the number of participants who scored above [N = 142] and below [N = 136] the mean). In the training set, we then used LASSO regression with 10 cross-validation folds to extract βs that corresponded to the λ at which the minimum MSE was achieved. First, we confirmed using robust linear regression that the only surviving brain region, L ITG, had a negative effect on IRI-PT both in the training set, $\beta = -0.003$ [95% CI: -0.005, -8.000e-04], $P_{Bon} = 0.011$, $R^2 = 0.035$, N = 223, and in the test set, $\beta = -0.005$ [95% CI: -0.008, -0.001], $P_{Bon} = 0.014$, $R^2 = 0.130$, N = 55 (*Figure 2*). We then confirmed using LASSO regression that the model trained solely on L ITG predicted IRI-PT in the test set, $P_p = 0.013$, $R^2 = 0.030$, N = 55 (*Figure 2*). Following the same procedure, we could not predict IRI-EC in the test, $P_p = 0.910$ (*Figure 2*; *Section S6*).

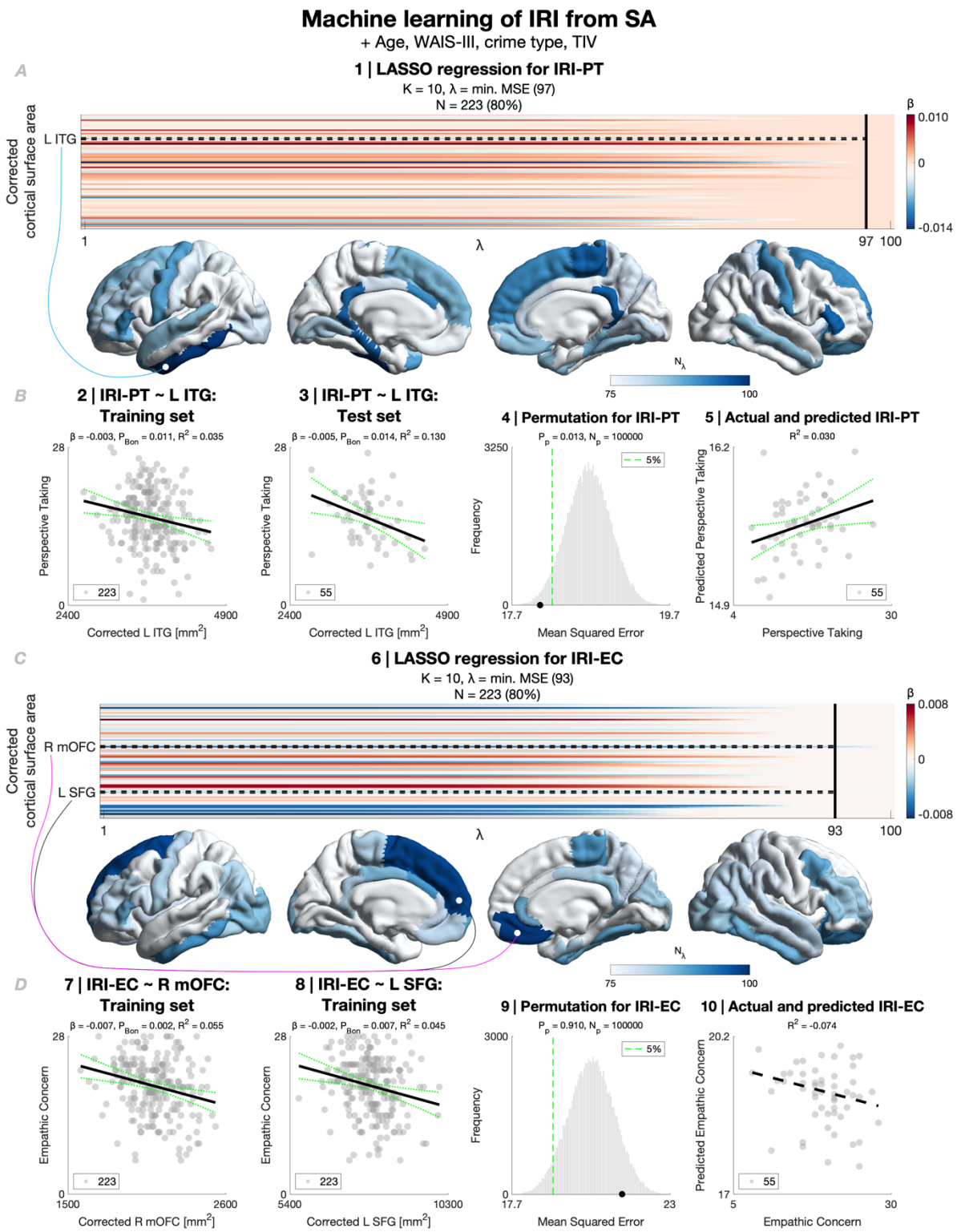

Figure 2 | Machine learning of IRI from SA. Panel A shows the cross-validated LASSO penalization of regional SA for IRI-PT. The cortical map represents the number of λs at which the brain region survived the LASSO penalization regardless of its coefficient's direction. In other words, mapped is the sum of instances – from 75 to 100, as shown in the legend – at which the regional coefficient remained a non-zero value. Panel B shows L-ITG SA explaining IRI-PT in the training and test sets, and its prediction of out-of-sample IRI-PT as assessed by a permutation test for MSE. Panels C and D repeat for IRI-EC the

steps described in panels A and B. Results were different compared to IRI-PT, such that the two brain regions that survived the LASSO penalization for IRI-EC, R mOFC and L SFG, explained it only in the training but not test set, nor did they predict out-of-sample IRI-EC. Ninety-five-percent confidence bounds in models 2, 3, 5, 7, and 8, and the significance threshold in models 4 and 9, are in dotted/dashed green. SA for these analyses was corrected for age, WAIS-III, crime type, and TIV.

Empathy and BigBrain gradient

Next, we tested the interaction effect between the two IRI scores and the five BigBrain bins, each representing covariate-corrected SA averaged across the brain regions within the bin (and Z-scored within the bin). We found an IRI-by-bin interaction for IRI-PT ($F[4, 1380] = 4.274$, $P_p = 0.004$, $N = 278$) but not IRI-EC ($P = 0.140$, $N = 278$). In particular, individuals with higher – but not lower – IRI-PT scores had a gradual reduction in SA from Bin 1 (sensorimotor) to Bin 5 (limbic) and reduced SA in Bin 5 compared to Bin 1 ($\beta_Z = -0.044$ [95% CI: -0.068, -0.021], $P_{Bon} = 0.009$, $N = 278$). When we grouped participants based on the mean and standard deviation, we also confirmed for IRI-PT a group-by-bin interaction ($F[4, 985] = 5.221$, $P_p = 0.001$, $N = 199$). In particular, the high-scoring group had a gradual reduction in SA from Bin 1 to Bin 5 and reduced SA in Bin 5 compared to Bin 1 ($\beta_Z = -0.533$ [95% CI: -0.803, -0.264], $P_{Bon} = 0.007$, $N = 199$), while the low-scoring group had the opposite profile, with SA increasing gradually from Bin 1 to Bin 5 (*Figure 3*). For IRI-EC, there was no group-by-bin interaction ($P = 0.061$, $N = 186$). See also *Section S7*.

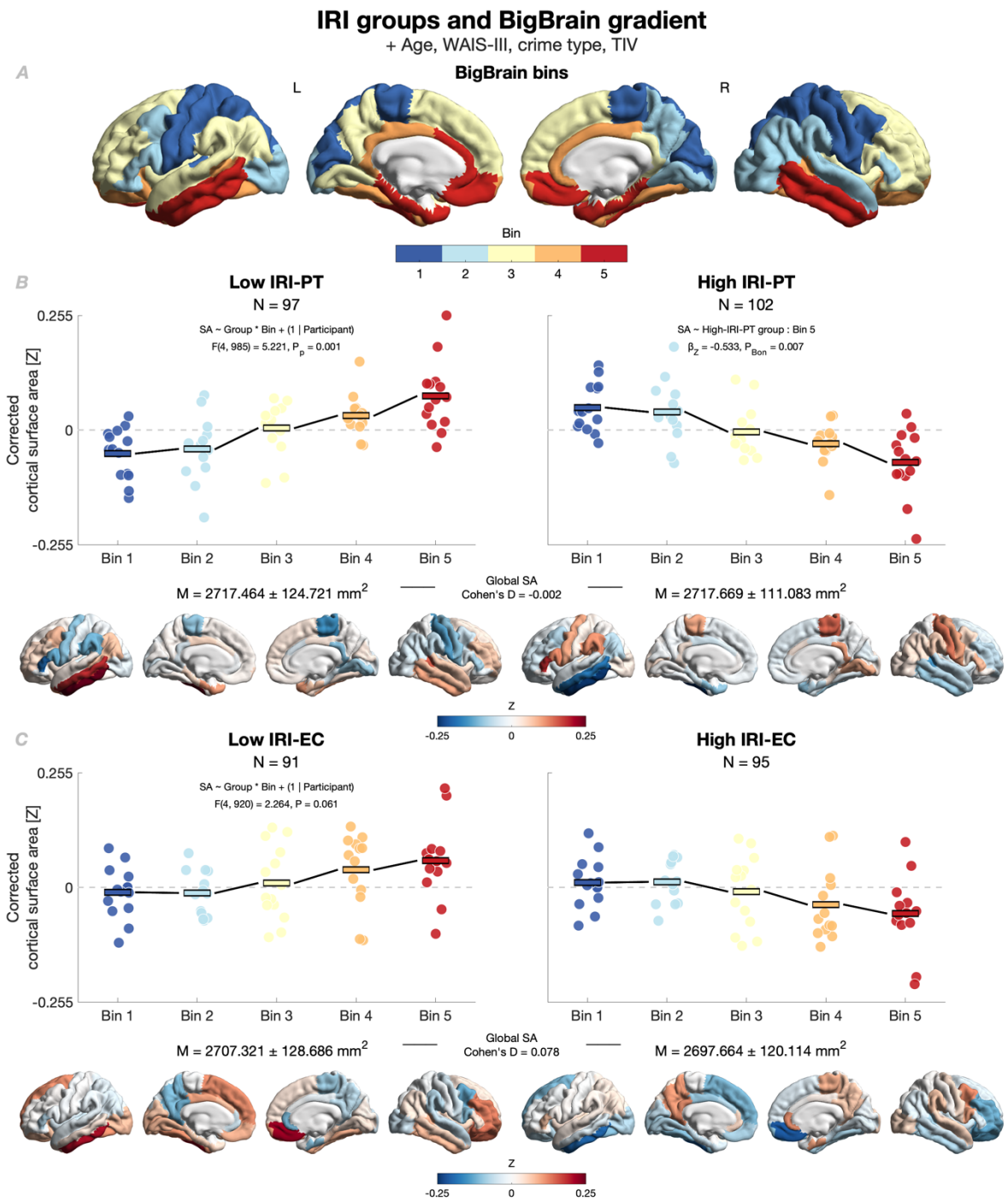

Figure 3 | IRI groups and BigBrain gradient. Panel A shows the division of the 68 Desikan-Killiany brain regions into the five BigBrain bins. Panel B shows a group-by-bin interaction for IRI-PT, with the high-scoring group having a gradual reduction in SA from Bin 1 (including areas with marked laminar differentiation, such as sensorimotor cortices) to Bin 5 (including areas with subtle laminar differentiation, such as limbic cortices). The high-scoring group also had reduced SA in Bin 5 compared to Bin 1. The low-scoring group had the opposite profile, with SA increasing gradually from Bin 1 to Bin 5. These effects occurred in the absence of a global SA difference (Cohen's D = -0.002). Panel C

shows no group-by-bin interaction for IRI-EC. Data points represent mean SA of the binned brain regions. SA for these analyses was corrected for age, WAIS-III, crime type, and TIV.

Psychopathy and global brain structure

Next, we tested global SA by psychopathy status. We found that psychopaths (N = 39) had increased global SA compared to non-psychopaths (N = 114), β = 55.887 [95% CI: 12.715, 99.059], P_p = 0.013, adj. R^2 = 0.719, Cohen's D = 0.480 (*Figure 4*). Four brain regions had a moderate Cohen's D: (1) left rostral middle frontal gyrus (Cohen's D = 0.737); (2) right fusiform gyrus (Cohen's D = 0.709); (3) left lateral orbitofrontal cortex (Cohen's D = 0.587); and (4) L ITG (Cohen's D = 0.560). We did not test the significance of each regional difference, as we had already treated L ITG as an ROI (*Figure 1*). Instead, we correlated these Cohen's Ds with the T-values for IRI-PT and IRI-EC plotted in *Figure 1*. There was a negative relationship for IRI-PT, ρ = -0.359, P_{Bon} = 0.006, and no relationship for IRI-EC, P = 0.120 (*Figure 4*).

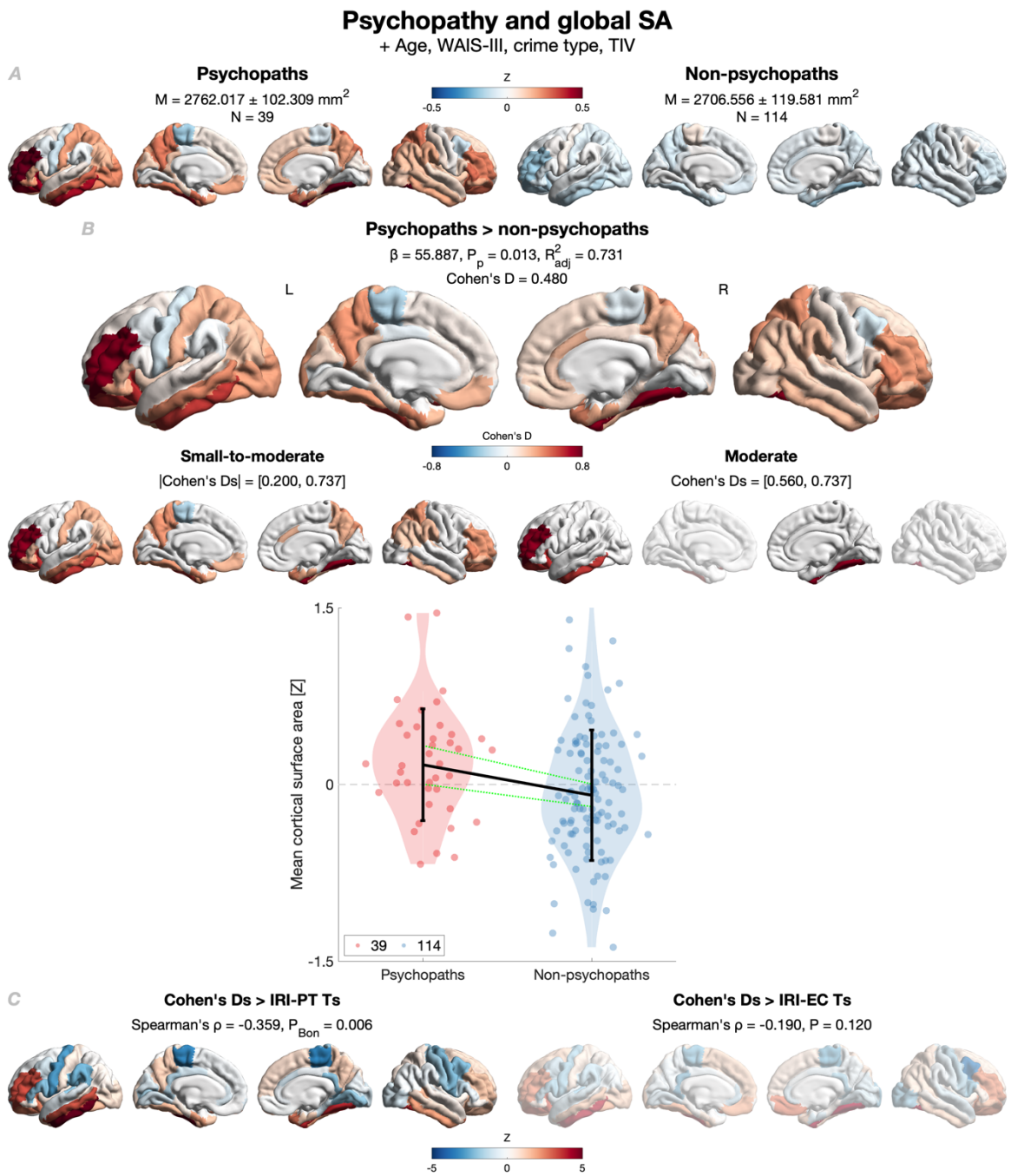

Figure 4 | Psychopathy and global SA. Panel A shows global SA separately in psychopaths and non-psychopaths, Z-scored across the groups. Panel B shows increased global SA in psychopaths. The smaller cortical maps were thresholded by removing brain regions with Cohen's Ds < |0.2| (on the left) and < 0.5 (on the right). In the violin plot, which includes a kernel-density estimation for each group, 95% confidence bounds are in dotted green and error bars represent standard deviation. This model controlled for age, WAIS-III, crime type, and TIV. Panel C shows a negative Spearman's correlation between the Cohen's Ds (plotted in panel B) and the T-values for IRI-PT but not IRI-EC (plotted in *Figure 1*). For visualization, each vector of values was Z-scored, the T-values were then subtracted from the Cohen's Ds, and the regional differences were mapped onto the cortical surface.

Psychopathy and structural covariance

Finally, as described in *Section S2*, we tested covariate-corrected SA covariance between psychopaths (N = 39) and non-psychopaths (N = 114). We found no group difference in global SA covariance, P_p = 0.395, or modularity count, N = 4 – although the modules showed descriptively less hemispheric symmetry in psychopaths (*Figure 5*). Neither did we find a group difference in global efficiency, P_p = 0.852, or in five other graph-theoretical metrics at the nodal level: local efficiency, $Ps_{FWE} \geq 0.440$; strength, $Ps_{FWE} \geq 0.263$; degree, $Ps_{FWE} \geq 0.530$; or betweenness centrality, $Ps_{FWE} \geq 0.328$. We did, however, find reduced covariance in psychopaths between the left precentral gyrus (L PG) and left isthmus-cingulate cortex (L ICC), Pearson's r-to-Z difference = -1.013, P_{FWE} = 9.500e-04 (*Figure 6*).

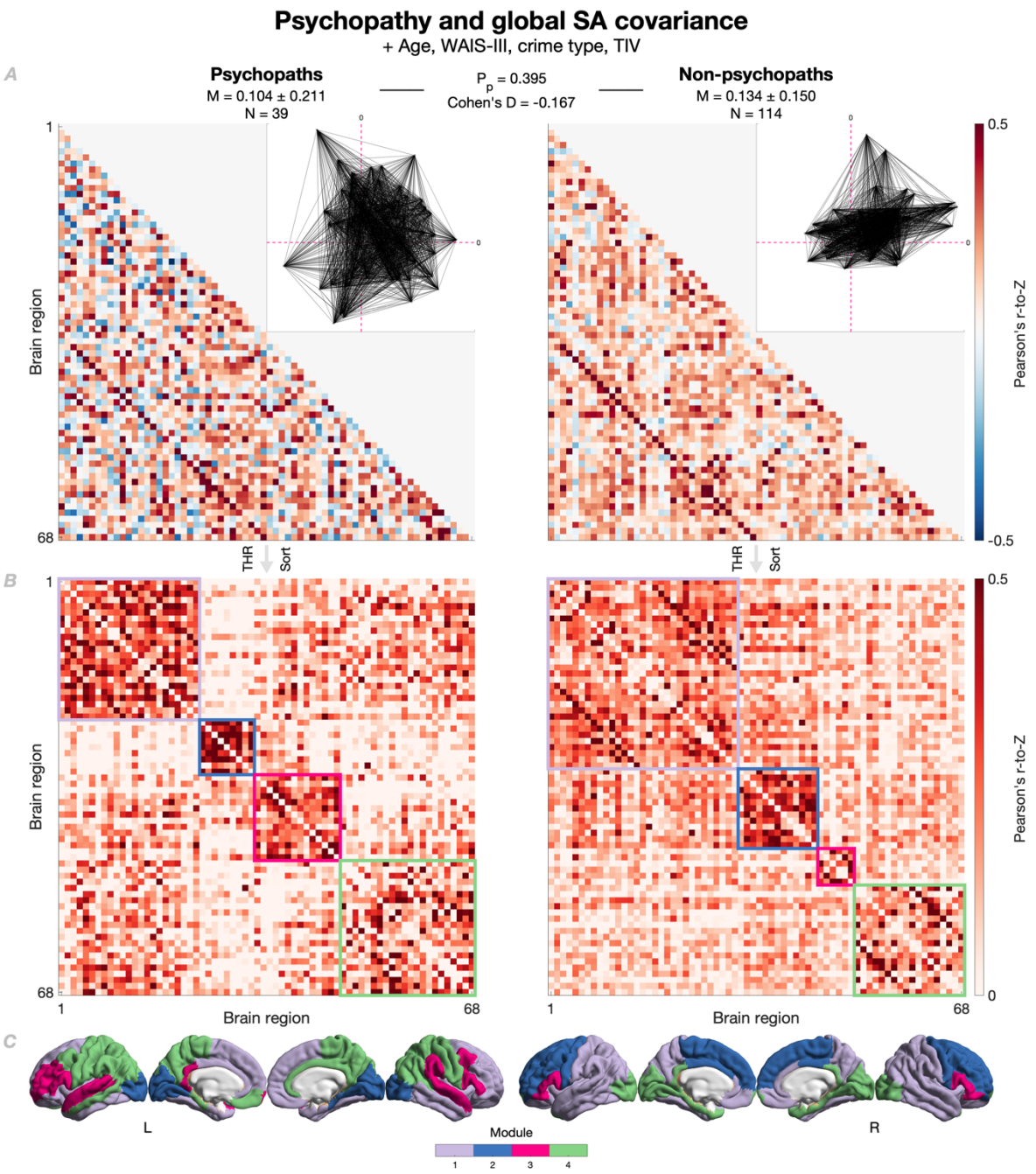

Figure 5 | Psychopathy and global SA covariance. Panel A shows raw SA-covariance matrices for psychopaths and non-psychopaths. There was no group difference in global SA covariance, only a tendency toward reduced and more deviated covariance in psychopaths. The top right corners of the matrices show dense adjacency graphs to aid visualization. Panel B shows SA-covariance matrices thresholded by removing negative edges and sorted by the module. There was no group difference in modularity count (N = 4). Panel C shows the modules plotted on the cortical surface. SA for these analyses was corrected for age, WAIS-III, crime type, and TIV.

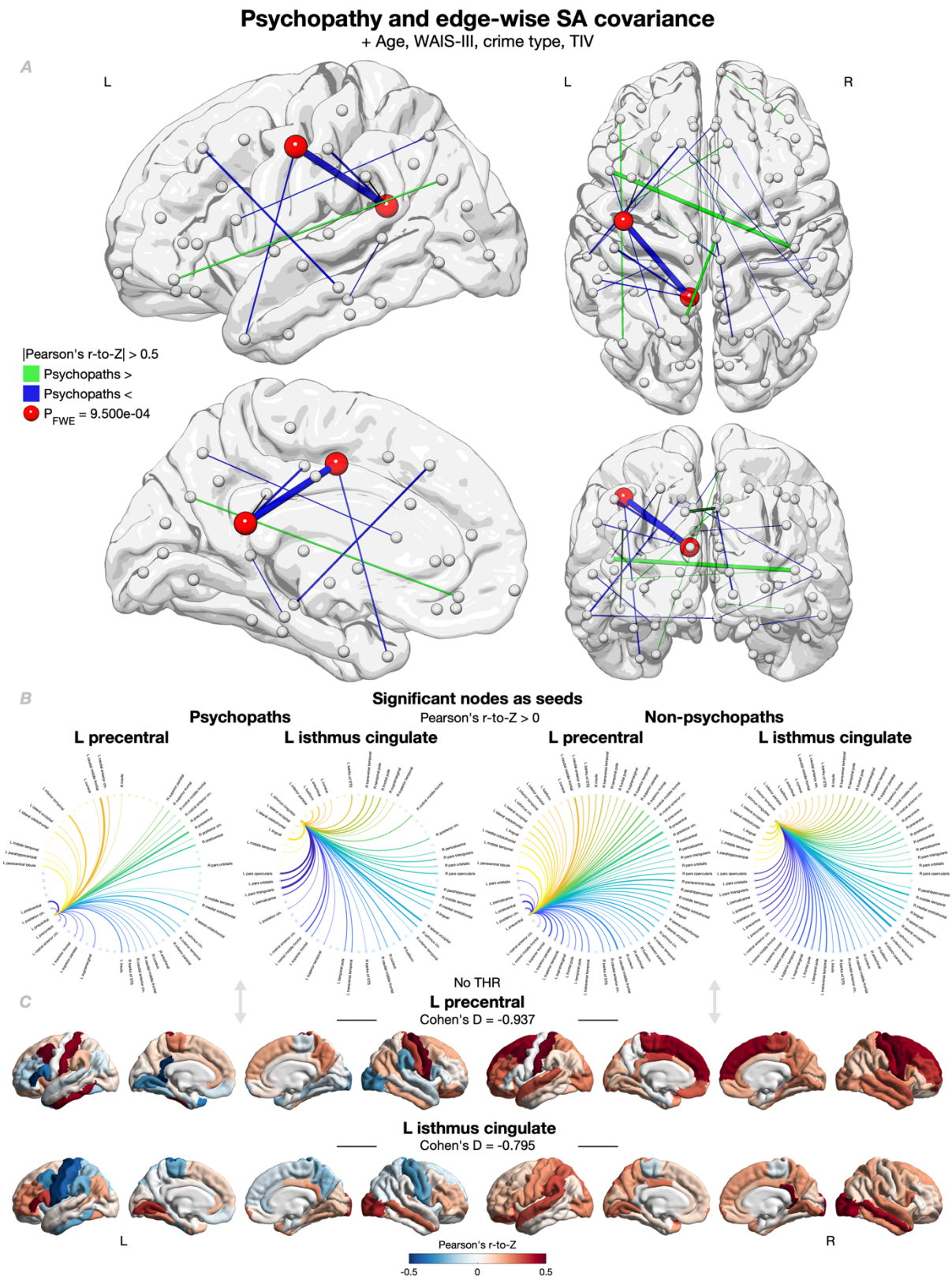

Figure 6 | Psychopathy and edge-wise SA covariance. Panel A shows reduced SA covariance between L PG and L ICC (the thickest blue edge with red orbs) in psychopaths (N = 39) compared to non-psychopaths (N = 114). The remaining edges in the plots passed the threshold |Pearson's r-to-Z| > 0.5, but did not survive the FWE correction. Panel B shows circular graphs for the two significant nodes as

seeds, with the graphs having been thresholded by removing negative edges and ordering brain regions in the FreeSurfer convention. Panel C shows unthresholded edges for the two seeds plotted on the cortical surface and compared between the groups using Cohen's D. SA for these analyses was corrected for age, WAIS-III, crime type, and TIV.

Discussion

In 278 White adult males from prison, we find that brain structure (as measured by MRI) reflects empathy (as measured by IRI) and psychopathy (as measured by PCL-R). In particular, L-ITG SA related negatively to IRI-PT and positively to PCL-R and PCL-R item 8 (Callousness/Lack of Empathy). L-ITG SA further predicted IRI-PT scores in an out-of-sample test, and, mapping onto the histological BigBrain gradient, higher IRI-PT scores entailed a progressive reduction in SA from Bin 1 (sensorimotor) to Bin 5 (limbic). None of these analyses yielded significance for IRI-EC. Furthermore, psychopaths had increased L-ITG SA as well as reduced IRI-PT and IRI-EC scores. Psychopaths also had increased global SA and reduced SA covariance between L PG and L ICC. There were no CT relationships with IRI-PT or IRI-EC, nor were there differences in psychopaths in global, modular, or nodal SA covariance. All of these brain effects were independent of age, intelligence, crime type, and brain size – for which the psychopaths and non-psychopaths were matched – and the effect of L ITG on IRI-PT was robust to a number of sensitivity analyses. We provide novel insights into the brain correlates of empathy and psychopathy in incarcerated males.

Across the univariate and multivariate analyses of empathy, we reliably identified only one brain region: L ITG. This brain region is known in the functional neuroimaging of cognitive empathy in the general population (e.g., Arioli et al., 2021; Diveica et al., 2021; Schurz et al., 2021). It falls in part within the limbic and default-mode networks, as defined by Yeo et al. (2011) (for the Desikan-Killiany atlas, see Grotzinger et al., 2023). Some of its portions (such as anterior; Ronconi et al., 2020) correlate with the terms “empathy”, “mentalizing”, and “theory mind” in the Neurosynth meta-analysis (e.g., https://neurosynth.org/analyses/terms/empathy/; Yarkoni et al., 2011). That we found any relationship between IRI and SA but not CT provides further evidence that SA is more sensitive than the latter to antisocial phenotypes (Carlisi et al., 2020). That we found any relationship between SA and IRI-PT but not IRI-EC agrees with the antisocial literature in that across these populations, cognitive empathy is reduced to a greater extent than affective empathy (Jolliffe & Farrington, 2004; Vachon et al., 2014; van Langen et al., 2014; Morrow, 2019; Campos et al., 2022), including when the two are measured with IRI-PT and IRI-EC, respectively (van Langen et al., 2014; Campos et al., 2022).

L ITG – but also R mOFC and L SFG, two other "empathic" brain regions (e.g., Schurz et al., 2021) that showed up for IRI-EC in our machine-learning analysis – are known in the antisocial literature as well. For instance, the biggest volumetric reduction in incarcerated homicide offenders was observed in a cluster encompassing L ITG, with another significant cluster encompassing R mOFC (Sajous-Turner et al., 2020). R mOFC was also found to be both structurally and functionally affected among antisocial populations in the first meta-analysis on the topic (Yang & Raine, 2009), extending work on its involvement in aggressive behavior (e.g., Pietrini et al., 2000; Coccaro et al., 2007; Beyer et al., 2014). A functional meta-analysis (Dugré & Potvin, 2021) revealed in antisocial individuals a negative relationship between the resting-state connectivity of the ventromedial prefrontal cortex and PCL-R Factor 2 (Chronic Antisocial), for which we also observed a trend in relation to L ITG in a follow-up analysis. Dorsal portions of the prefrontal cortex are similarly known to be affected among these populations (Yang & Raine, 2009; Rogers & De Brito, 2016; Dugré & Potvin, 2021). From a neuropsychological perspective, damage to the left temporal cortex was shown to be associated with diminished empathy (Driscoll et al., 2012). As L ITG was ranked fourth out of 68 brain regions in terms of Cohen's D, and it related in the *opposite* direction to IRI-PT and PCL-R in the entire sample, it could constitute a brain-structural correlate of pervasively reduced/impaired empathy in psychopaths (e.g., Campos et al., 2022). It could play a role in this empathic reduction/impairment alongside other brain regions, as further suggested by our analysis of the BigBrain gradient (Pacquola et al., 2019) and a negative correlation between the "psychopathic" Cohen's D map and the "empathic" T map across the cortex.

The most affected brain region in psychopaths was the left rostral middle frontal gyrus. Compared to the three aforementioned brain regions, this one is much less known in the empathy literature. Partly covering the dorsolateral prefrontal cortex in the Desikan-Killiany atlas, it is rather involved in cognitive control and inhibition (Friedman & Robbins, 2022), serving to constrain impulsivity, with the latter trait being another remarkable feature of psychopaths (De Brito et al., 2021a). The fact that L ITG was not the most affected brain region could thus suggest that reduced/impaired empathy only partly paints the psychopathic picture. In fact, merely one out of the 20 PCL-R/YV traits directly relates to empathy (item 8, Callousness/Lack of Empathy) while at least three to impulsivity or ADHD-like traits in general (item 3, Need of Stimulation/Proneness to Boredom; item 10, Poor Behavioral Control; item 14, Impulsivity) (American Psychiatric Association, 2013). Tying impulsivity to brain structure

in patients with traumatic brain injury, one lesion-symptom-mapping study identified within the left prefrontal cortex a cluster associated specifically with motor impulsivity, defined as "acting without thinking" (McDonald et al., 2017). Perhaps interestingly, heightened global impulsivity was associated with damage not only to the prefrontal cortex but also L ITG.

Just as L-ITG SA was increased in psychopaths, so was SA across the cortex. Intuitively, this may go against the literature, which most commonly reports volumetric reductions among antisocial populations (e.g., Rogers & De Brito, 2016; De Brito et al., 2021b; Tully et al., 2023), and SA scales positively with brain volume (Toro et al., 2008). However, given the negative relationship between IRI-PT and SA, the "inflated-antisocial-brain" effect (already documented in prison; Korponay et al., 2017) would be expected, as psychopaths scored lower on IRI-PT. Furthermore, one meta-analysis confirmed increased volume of the right fusiform gyrus among antisocial populations (Aoki et al., 2014) – as we did in psychopaths for SA – and frontal-temporal-parietal SA was also reported to be increased in antisocial-personality individuals (Jiang et al., 2016). As both psychopaths and non-psychopaths in our sample were incarcerated, they represent exclusively the antisocial population, which restricts comparisons to the general-population literature. What adds further complication is that the relationship between a psychological and a brain-structural variable could vary by psychopathy status (Korponay & Koenigs, 2021).

While global SA in psychopaths was increased, edge-wise SA covariance – for L PG and L ICC – was reduced. This finding adds to the covariance analyses in psychopaths based on CT (Yang et al., 2012) and functional connectivity (Espinoza et al., 2018), suggesting that a better understanding of reduced/impaired empathy in psychopaths (as well as their other traits) may lie not only in the structure or function of particular brain regions but also in multimodal relationships between them.

The first limitation of our study would be the use of a self-report measure in an antisocial population, as repeated lying characterizes antisocial personality (American Psychiatric Association, 2013). However, apart from self-report being the standard empathy measurement (de Lima & de Lima Osório, 2021), we confirmed the effect of L ITG on IRI-PT using a non-self-report measure of empathy being PCL-R item 8 (Callousness/Lack of Empathy) as well as among those who scored 0 on PCL-R item 4 (Pathological Lying) and who did not meet the psychopathy criteria. Another relevant point to consider is that empathy as defined by the two IRI subscales has a constrained meaning. For instance, IRI-EC could be

more accurately viewed as a measure of compassion (feeling *for* others) rather than affective empathy in the sense of affect sharing (feeling *with* others), with the two being potentially dissociable in the brain (Singer & Klimecki, 2014; Preckel et al., 2018; Kim et al., 2020). Nevertheless, it is common to view IRI-EC as a measure of affective empathy (e.g., Vachon et al., 2014), and other popular empathy tasks may similarly tap onto both compassion and affect sharing (e.g., Baron-Cohen & Wheelwright, 2004). Stepping beyond the scope of this paper, theoretical (Bloom, 2017a; Bloom, 2017b; Zaki, 2017) and methodological (Israelashvili et al., 2019; Murphy & Lilienfeld, 2019) disagreement persists.

Secondly, although 278 participants may constitute a respectably sized sample in structural (Button et al., 2013) and psychiatric (Fusar-Poli et al., 2013) neuroimaging, we were likely still underpowered to identify all true effects (Cecchetti & Handjaras, 2022). Thirdly, while incarcerated individuals are well-evidenced to have reduced/impaired empathy (e.g., Joliffe & Farrington, 2004; van Langen et al., 2014; Campos et al., 2022), including a community sample for comparison would be advantageous. Fourthly, we did not have prison time, substance abuse, or psychiatric diagnoses to control for. However, we did have this information for 125 participants in the brain-structural sample, and we did not confirm the importance of these covariates. Although neither did we confirm the importance of impulsivity in 212 out of the 278 participants, controlling for other psychological covariates in the entire sample could also be advantageous – variables such as depression symptoms or Big-Five personality traits, which were found to reflect cognitive empathy in a male population (Radecki et al., 2019). Finally, our effects cannot be generalized to females, who typically score higher than males in both self-reported (Christov-Moore et al., 2014; Greenberg et al., 2018; Archer, 2019) and tested (Olderbak et al., 2019; Baron-Cohen et al., 2022; Greenberg et al., 2023) empathy. Female neural correlates of empathy could therefore differ in magnitude, location, and even direction, as has been suggested for personality in the general population (Nostro et al., 2017).

Conclusions

We provide novel evidence in incarcerated males that L-ITG SA may relate in the *opposite* direction to empathy (negative) and psychopathy (positive), and that empathy can be predicted from brain structure alone and mapped onto a histological gradient. We further add to an emerging literature on differences – and in some cases, similarities – between psychopaths and non-psychopaths in brain structure and its covariance. Future work should employ not only structural but also diffusion-weighted and functional neuroimaging to investigate empathy and psychopathy in even larger samples of incarcerated males alongside controls. It should further investigate them in community-dwelling antisocial males and other relevant populations, including antisocial females and children/adolescents at risk of developing antisocial personality.

Declaration of interest

None.

Author contributions

Marcin A. Radecki: Conceptualization; Methodology; Formal analysis; Visualization; Writing – original draft; Writing – review & editing.

Erika Sampaolo: Conceptualization; Methodology; Writing – review & editing.

Giada Lettieri: Conceptualization; Methodology; Writing – review & editing.

Giacomo Handjaras: Conceptualization; Methodology; Writing – review & editing.

Carla L. Harenski: Conceptualization; Methodology; Data curation; Project administration; Writing – review & editing.

Sara Palumbo: Conceptualization; Data curation; Writing – review & editing.

Silvia Pellegrini: Conceptualization; Data curation; Writing – review & editing.

Pietro Pietrini: Conceptualization; Writing – review & editing.

Kent A. Kiehl: Conceptualization; Methodology; Data curation; Project administration; Funding acquisition; Supervision; Writing – review & editing.

Luca Cecchetti: Conceptualization; Methodology; Formal analysis; Supervision; Writing – review & editing.

Data and code availability

Data may become available under a data-use agreement. If interested, please contact Kent A. Kiehl at kkiehl@mrn.org. We shared the code for statistical analysis on OSF at https://osf.io/xazf6/?view_only=b9652ff8801b489a9520ad7b165d592a.

Acknowledgements

Giada Lettieri was supported by Marie Curie programme grant funding H2020, grant #101026032.

References

American Psychiatric Association, DSM-5 Task Force, 2013. *Diagnostic and Statistical Manual of Mental Disorders: DSM-5™ (5th ed.).* American Psychiatric Association Publishing, Washington, DC.

Amunts, K., Lepage, C., Borgeat, L., Mohlberg, H., Dickscheid, T., Rousseau, M.-E., … Evans, A.C., 2013. BigBrain: An ultrahigh-resolution 3D human brain model. *Science 340*(6139), 1472–1475.https://doi.org/10.1126/science.1235381

Andrews-Hanna, J.R., Saxe, R., Yarkoni, T., 2014. Contributions of episodic retrieval and mentalizing to autobiographical thought: Evidence from functional neuroimaging, resting-state connectivity, and fMRI meta-analyses. *NeuroImage 91,* 324–335. https://doi.org/10.1016/j.NeuroImage.2014.01.032

Aoki, Y., Inokuchi, R., Nakao, T., Yamasue, H., 2014. Neural bases of antisocial behavior: A voxel-based meta-analysis. *Soc. Cogn. Affect. Neurosci. 9*(8), 1223–1231. https://doi.org/10.1093/scan/nst104

Archer, J., 2019. The reality and evolutionary significance of human psychological sex differences. *Biol. Rev. 94*(4), 1381–1415. https://doi.org/10.1111/brv.12507

Arioli, M., Cattaneo, Z., Ricciardi, E., Canessa, N., 2021. Overlapping and specific neural correlates for empathizing, affective mentalizing, and cognitive mentalizing: A coordinate-based meta-analytic study. *Hum. Brain Mapp. 42*(14), 4777–4804. https://doi.org/10.1002/hbm.25570

Banissy, M.J., Kanai, R., Walsh, V., Rees, G., 2012. Inter-individual differences in empathy are reflected in human brain structure. *NeuroImage 62*(3), 2034–2039. https://doi.org/10.1016/j.NeuroImage.2012.05.081

Baron-Cohen, S., Radecki, M.A., Greenberg, D.M., Warrier, V., Holt, R.J., Allison, C., 2022. Sex differences in theory of mind: The on-average female advantage on the Reading the Mind in the Eyes Test. *Dev. Med. Child. Neurol. 64*(12), 1440–1441. https://doi.org/10.1111/dmcn.15364

Baron-Cohen, S., Wheelwright, S., 2004. The Empathy Quotient: An investigation of adults with Asperger syndrome or high functioning autism, and normal sex differences. *J. Autism Dev. Disord. 34*(2), 163–175. https://doi.org/10.1023/B:JADD.0000022607.19833.00

Beyer, F., Münte, T.F., Göttlich, M., Krämer, U.M., 2014. Orbitofrontal cortex reactivity to angry facial expression in a social interaction correlates with aggressive behavior. *Cerebral Cortex, 25*(9), 3057–3063. https://doi.org/10.1093/cercor/bhu101

Blair, R.J.R., Mitchell, D.G.V., Peschardt, K.S., Colledge, E., Leonard, R.A., Shine, J.H., … Perrett, D.I., 2004. Reduced sensitivity to others' fearful expressions in psychopathic individuals. *Pers. Individ. Differ. 37*(6), 1111–1122. https://doi.org/10.1016/j.paid.2003.10.008

Bloom, P., 2017a. Empathy and its discontents. *Trends Cogn. Sci. 21*(1), 24–31. https://doi.org/10.1016/j.tics.2016.11.004

Bloom, P., 2017b. Empathy, schmempathy: Response to Zaki. *Trends Cogn. Sci. 21*(2), 60–61. https://doi.org/10.1016/j.tics.2016.12.003

Burghart, M., Mier, D., 2022. No feelings for me, no feelings for you: A meta-analysis on alexithymia and empathy in psychopathy. *Pers. Individ. Differ. 194*(4), 111658. https://doi.org/10.1016/j.paid.2022.111658

Button, K.S., Ioannidis, J.P.A., Mokrysz, C., Nosek, B.A., Flint, J., Robinson, E.S.J., Munafò, M.R., 2013. Power failure: Why small sample size undermines the reliability of neuroscience. *Nat. Rev. Neurosci. 14*(5), 365–376. https://doi.org/10.1038/nrn3475

Bzdok, D., Schilbach, L., Vogeley, K., Schneider, K., Laird, A.R., Langner, R., Eickhoff, S.B., 2012. Parsing the neural correlates of moral cognition: ALE meta-analysis on morality, theory of mind, and empathy. *Brain Struct. Funct. 217*(4), 783–796. https://doi.org/10.1007/s00429-012-0380-y

Caldwell, B.M., Anderson, N.E., Harenski, K.A., Sitney, M.H., Caldwell, M.F., Van Rybroek, G. J., Kiehl, K.A., 2019. The structural brain correlates of callous-unemotional traits in incarcerated male adolescents. *NeuroImage Clin. 22,* 101703. https://doi.org/10.1016/j.nicl.2019.101703

Campos, C., Pasion, R., Azeredo, A., Ramião, E., Mazer, P., Macedo, I., Barbosa, F., 2022. Refining the link between psychopathy, antisocial behavior, and empathy: A meta-analytical approach across different conceptual frameworks. *Clin. Psychol. Rev. 94*, 102145. https://doi.org/10.1016/j.cpr.2022.102145

Carlisi, C.O., Moffitt, T.E., Knodt, A.R., Harrington, H., Ireland, D., Melzer, T.R., … Viding, E., 2020. Associations between life-course-persistent antisocial behaviour and brain structure in a population-representative longitudinal birth cohort. *Lancet Psychiatry 7*(3), 245–253. https://doi.org/10.1016/s2215-0366(20)30002-x

Cecchetti, L., Handjaras, G., 2022. Reproducible brain-wide association studies do not necessarily require thousands of individuals. *PsyArXiv.* https://doi.org/10.31234/osf.io/c8xwe

Chang, L.J., Jolly, E., Cheong, J.H., Rapuano, K.M., Greenstein, N., Chen, P.-H.A., Manning, J.R., 2021. Endogenous variation in ventromedial prefrontal cortex state dynamics during naturalistic viewing reflects affective experience. *Sci. Adv. 7*(17), eabf7129. https://doi.org/10.1126/sciadv.abf7129

Christov-Moore, L., Simpson, E.A., Coudé, G., Grigaityte, K., Iacoboni, M., & Ferrari, P.F., 2014. Empathy: Gender effects in brain and behavior. *Neurosci. Biobehav. Rev.* 46(4), 604–627. https://doi.org/10.1016/j.neubiorev.2014.09.001

Coccaro, E.F., McCloskey, M.S., Fitzgerald, D.A., Phan, K.L., 2007. Amygdala and orbitofrontal reactivity to social threat in individuals with impulsive aggression. *Biol. Psychiatry 62*(2), 168–178. https://doi.org/10.1016/j.biopsych.2006.08.024

Davis, M.H., 1980. A multidimensional approach to individual differences in empathy. *JSAS 10,* 85.

Davis, M.H., 1983. Measuring individual differences in empathy: Evidence for a multidimensional approach. *J. Pers. Soc. Psychol. 44*(1), 113–126. https://doi.org/10.1037/0022-3514.44.1.113

Dawel, A., O'Kearney, R., McKone, E., Palermo, R., 2012. Not just fear and sadness: Meta-analytic evidence of pervasive emotion recognition deficits for facial and vocal expressions in psychopathy. *Neurosci. Biobehav. Rev. 36*(10), 2288–2304. https://doi.org/10.1016/j.neubiorev.2012.08.006

De Brito, S.A., Forth, A.E., Baskin-Sommers, A.R., Brazil, I.A., Kimonis, E.R., Pardini, D., … Viding, E., 2021a. Psychopathy. *Nat. Rev. Dis. Primers 7*(1), 49. https://doi.org/10.1038/s41572-021-00282-1

De Brito, S.A., McDonald, D., Camilleri, J.A., Rogers, J.C., 2021b. Cortical and subcortical gray matter volume in psychopathy: A voxel-wise meta-analysis. *J. Abnorm. Psychol. 130*(6), 627–640. https://doi.org/10.1037/abn0000698

de Lima, F.F., de Lima Osório, F., 2021. Empathy: Assessment instruments and psychometric quality – A systematic literature review with a meta-analysis of the past ten years. *Front. Psychol. 12,* 781346. https://doi.org/10.3389/fpsyg.2021.781346

Deming, P., Dargis, M., Haas, B. W., Brook, M., Decety, J., Harenski, C., … Kosson, D.S., 2020. Psychopathy is associated with fear-specific reductions in neural activity during affective perspective-taking. *NeuroImage 223,* 117342. https://doi.org/10.1016/j.NeuroImage.2020.117342

Deming, P., Koenigs, M., 2020. Functional neural correlates of psychopathy: A meta-analysis of MRI data. *Transl. Psychiatry. 10*(1), 133. https://doi.org/10.1038/s41398-020-0816-8

Desikan, R.S., Ségonne, F., Fischl, B., Quinn, B.T., Dickerson, B.C., Blacker, D., … Killiany, R.J., 2006. An automated labeling system for subdividing the human cerebral cortex on MRI scans into gyral based regions of interest. *NeuroImage 31*(3), 968–980. https://doi.org/10.1016/j.NeuroImage.2006.01.021

Diveica, V., Koldewyn, K., Binney, R.J., 2021. Establishing a role of the semantic control network in social cognitive processing: A meta-analysis of functional neuroimaging studies. *NeuroImage 245,* 118702. https://doi.org/10.1016/j.NeuroImage.2021.118702

Drayton, L.A., Santos, L.R., Baskin-Sommers, A., 2018. Psychopaths fail to automatically take the perspective of others. *Proc. Natl. Acad. Sci. U.S.A. 115*(13), 3302–3307. https://doi.org/10.1073/pnas.1721903115

Driscoll, D.M., Dal Monte, O., Solomon, J., Krueger, F., Grafman, J., 2012. Empathic deficits in combat veterans with traumatic brain injury. *Cogn. Behav. Neurol. 25*(4), 160–166. https://doi.org/10.1097/wnn.0b013e318280cf4e

Dugré, J.R., Potvin, S., 2021. Impaired attentional and socio-affective networks in subjects with antisocial behaviors: A meta-analysis of resting-state functional connectivity studies. *Psychol. Med. 51*(8), 1249–1259. https://doi.org/10.1017/S0033291721001525

Eres, R., Decety, J., Louis, W.R., Molenberghs, P., 2015. Individual differences in local gray matter density are associated with differences in affective and cognitive empathy. *NeuroImage 117,* 305–310. https://doi.org/10.1016/j.NeuroImage.2015.05.038

Espinoza, F.A., Vergara, V.M., Reyes, D., Anderson, N.E., Harenski, C.L., Decety, J., … Calhoun, V.D. (2018). Aberrant functional network connectivity in psychopathy from a large (N = 985) forensic sample. *Hum. Brain Mapp. 39*(6), 2624–2634. https://doi.org/10.1002/hbm.24028

Fallon, N., Roberts, C., Stancak, A., 2020. Shared and distinct functional networks for empathy and pain processing: A systematic review and meta-analysis of fMRI studies. *Soc. Cogn. Affect. Neurosci. 15*(7), 709–723. https://doi.org/10.1093/scan/nsaa090

Fan, Y., Duncan, N.W., de Greck, M., Northoff, G., 2011. Is there a core neural network in empathy? An fMRI based quantitative meta-analysis. *Neurosci. Biobehav. Rev. 35*(3), 903–911. https://doi.org/10.1016/j.neubiorev.2010.10.009

Fede, S.J., Borg, J.S., Nyalakanti, P.K., Harenski, C.L., Cope, L.M., Sinnott-Armstrong, W., … Kiehl, K.A. (2016). Distinct neuronal patterns of positive and negative moral processing in psychopathy. *Cogn. Affect. Behav. Neurosci.* 16(6), 1074–1085. https://doi.org/10.3758/s13415-016-0454-z

First, M.B., Gibbon, M., 2004. *The Structured Clinical Interview for DSM-IV Axis I Disorders (SCID-I) and the Structured Clinical Interview for DSM-IV Axis II Disorders (SCID-II)*, in: Hilsenroth, M.J., Segal, D.L. (Eds.), Comprehensive Handbook of Psychological Assessment: Vol. 2. Personality Assessment. John Wiley & Sons, Inc., Hoboken, pp. 134–143.

Fischl, B., 2012. FreeSurfer. *NeuroImage 62*(2), 774–781. https://doi.org/10.1016/j.NeuroImage.2012.01.021

Forth, A.E., Kosson, D.S., Hare, R.D., 2003. *Hare Psychopathy Checklist: Youth Version.* Multi-Health Systems, Toronto.

Friedman, N.P., Robbins, T.W., 2022. The role of prefrontal cortex in cognitive control and executive function. *Neuropsychopharmacol. 47,* 72–89. https://doi.org/10.1038/s41386-021-01132-0

Fusar-Poli, P., Radua, J., Frascarelli, M., Mechelli, A., Borgwardt, S., Di Fabio, F., … David, S.P., 2013. Evidence of reporting biases in voxel-based morphometry (VBM) studies of psychiatric and neurological disorders. *Hum. Brain Mapp. 35*(7), 3052–3065. https://doi.org/10.1002/hbm.22384

Glasser, M.F., Sotiropoulos, S.N., Wilson, J.A., Coalson, T.S., Fischl, B., Andersson, J.L., … The WU-Minn HCP Consortium, 2013. The minimal preprocessing pipelines for the Human Connectome Project. *NeuroImage 80,* 105–124. https://doi.org/10.1016/j.NeuroImage.2013.04.127

Greenberg, D.M., Warrier, V., Allison, C., Baron-Cohen, S., 2018. Testing the Empathizing-Systemizing theory of sex differences and the Extreme Male Brain theory of autism in half a million people. *Proc. Natl. Acad. Sci. U. S. A. 115*(48), 12152–12157. https://doi.org/10.1073/pnas.1811032115

Greenberg, D.M., Warrier, V., Abu-Akel, A.M., Allison, C., Gajos, K.Z., Reinecke, K., … Baron-Cohen, S., 2023. Sex and age differences in "theory of mind" across 57 countries using the English version of the "Reading the Mind in the Eyes" Test. *Proc. Natl. Acad. Sci. U.S.A. 120*(1), e2022385119. https://doi.org/10.1073/pnas.2022385119

Grotzinger, A.D., Mallard, T.T., Liu, Z., Seidlitz, J., Ge, T., Smoller, J. W., 2023. Multivariate genomic architecture of cortical thickness and surface area at multiple levels of analysis. *Nat. Commun.* 14, 946. https://doi.org/10.1038/s41467-023-36605-x

Hare, R.D., 1991. *Hare Psychopathy Checklist–Revised.* Multi-Health Systems, Toronto.

Hare, R.D., 2003. *Hare Psychopathy Checklist–Revised, second ed.* Multi-Health Systems, Toronto.

Harenski, C.L., Calhoun, V.D., Bustillo, J.R., Haas, B.W., Decety, J., Harenski, K.A., … Kiehl, K.A., 2018. Functional connectivity during affective mentalizing in criminal offenders with psychotic disorders: Associations with clinical symptoms. *Psychiatry Res. Neuroimaging* 271, 91–99. https://doi.org/10.1016/j.pscychresns.2017.11.003

Huntenburg, J.M., Bazin, P.-L., Margulies, D.S., 2018. Large-scale gradients in human cortical organization. *Trends Cogn. Sci.* *22*(1), 21–31. https://doi.org/10.1016/j.tics.2017.11.002

Israelashvili, J., Sauter, D., Fischer, A., 2019. How well can we assess our ability to understand others' feelings? Beliefs about taking others' perspectives and actual understanding of others' emotions. *Front. Psychol.* *10,* 2475. https://doi.org/10.3389/fpsyg.2019.02475

Jalava, J., Griffiths, S., Larsen, R.R., Alcott, B.E., 2021. Is the psychopathic brain an artifact of coding bias? A systematic review. *Front. Psychol.* *12,* 654336. https://doi.org/10.3389/fpsyg.2021.654336

Jauniaux, J., Khatibi, A., Rainville, P., Jackson, P.L., 2019. A meta-analysis of neuroimaging studies on pain empathy: Investigating the role of visual information and observers' perspective. *Soc. Cogn. Affect. Neurosci.* *14*(8), 789–813. https://doi.org/10.1093/scan/nsz055

Jenkinson, M., Beckmann, C.F., Behrens, T.E.J., Woolrich, M.W., Smith, S.M., 2012. FSL. *NeuroImage 62*(2), 782–790. https://doi.org/10.1016/j.NeuroImage.2011.09.015

Jiang, W., Li, G., Liu, H., Shi, F., Wang, T., Shen, C., … Shen, D. (2016). Reduced cortical thickness and increased surface area in antisocial personality disorder. *Neuroscience, 337,* 143–152. https://doi.org/10.1016/j.neuroscience.2016.08.052

Johanson, M., Vaurio, O., Tiihonen, J., Lähteenvuo, M., 2020. A systematic literature review of neuroimaging of psychopathic traits. *Front. Psychiatry 10,* 1027. https://doi.org/10.3389/fpsyt.2019.01027

Johnson, B.N., Kivity, Y., Rosenstein, L.K., LeBreton, J.M., Levy, K.N., 2022. The association between mentalizing and psychopathology: A meta-analysis of the reading the mind in the eyes task across psychiatric disorders. *Clin. Psychol. 29*(4), 423–439. https://doi.org/10.1037/cps0000105

Jolliffe, D., Farrington, D.P., 2004. Empathy and offending: A systematic review and meta-analysis. *Aggress. Violent Behav. 9*(5), 441–476. https://doi.org/10.1016/j.avb.2003.03.001

Keysers, C., Gazzola, V., 2014. Dissociating the ability and propensity for empathy. *Trends Cogn. Sci. 18*(4), 163–166. https://doi.org/10.1016/j.tics.2013.12.011

Kim, J.J., Cunnington, R., Kirby, J.N., 2020. The neurophysiological basis of compassion: An fMRI meta-analysis of compassion and its related neural processes. *Neurosci. Biobehav. Rev. 108,* 112–123. https://doi.org/10.1016/j.neubiorev.2019.10.023

Korponay, C., Pujara, M., Deming, P., Philippi, C., Decety, J., Kosson, D.S., … Koenigs, M., 2017. Impulsive-antisocial psychopathic traits linked to increased volume and functional connectivity within prefrontal cortex. *Soc. Cogn. Affect. Neurosci. 12*(7), 1169–1178. https://doi.org/10.1093/scan/nsx042

Korponay, C., Koenigs, M., 2021. Gray matter correlates of impulsivity in psychopathy and in the general population differ by kind, not by degree: A comparison of systematic

reviews. *Soc. Cogn. Affect. Neurosci.* *16*(7), 683–695. https://doi.org/10.1093/scan/nsab045

Lamm, C., Decety, J., Singer, T., 2011. Meta-analytic evidence for common and distinct neural networks associated with directly experienced pain and empathy for pain. *NeuroImage 54*(3), 2492–2502. https://doi.org/10.1016/j.NeuroImage.2010.10.014

Larivière, S., Paquola, C., Park, B.-Y., Royer, J., Wang, Y., Benkarim, O., … Bernhardt, B.C., 2021. The ENIGMA Toolbox: Multiscale neural contextualization of multisite neuroimaging datasets. *Nat. Methods 18*(7), 698–700. https://doi.org/10.1038/s41592-021-01186-4

Mar, R.A., 2011. The neural bases of social cognition and story comprehension. *Annu. Rev. Psychol. 62,* 103–134. http://doi.org/10.1146/annurev-psych-120709-145406

Margulies, D.S., Ghosh, S.S., Goulas, A., Falkiewicz, M., Huntenburg, J.M., Langs, G., … Smallwood, J., 2016. Situating the default-mode network along a principal gradient of macroscale cortical organization. *Proc. Natl. Acad. Sci. U.S.A. 113*(44), 12574–12579. https://doi.org/10.1073/pnas.1608282113

Marsh, A.A., Blair, R.J.R., 2008. Deficits in facial affect recognition among antisocial populations: A meta-analysis. *Neurosci. Biobehav. Rev. 32*(3), 454–465. https://doi.org/10.1016/j.neubiorev.2007.08.003

McDonald, V., Hauner, K. K., Chau, A., Krueger, F., Grafman, J. 2017. Networks underlying trait impulsivity: Evidence from voxel-based lesion-symptom mapping. *Hum. Brain Mapp. 38*(2), 656–665. https://doi.org/10.1002/hbm.23406

Miller, P.A., Eisenberg, N., 1988. The relation of empathy to aggressive and externalizing/antisocial behavior. *Psychol. Bull. 103*(3), 324–344. https://doi.org/10.1037/0033-2909.103.3.324

Molenberghs, P., Johnson, H., Henry, J.D., Mattingley, J.B., 2016. Understanding the minds of others: A neuroimaging meta-analysis. *Neurosci. Biobehav. Rev. 65,* 276–291. https://doi.org/10.1016/j.neubiorev.2016.03.020

Morrow, E.P., 2019. Cognitive, affective, and general empathy in individuals convicted of a sexual offense: A meta-analysis. *Sex. Abuse 32*(8), 883–906. https://doi.org/10.1177/1079063219858062

Murphy, B.A., Lilienfeld, S.O., 2019. Are self-report cognitive empathy ratings valid proxies for cognitive empathy ability? Negligible meta-analytic relations with behavioral task performance. *Psychol. Assess. 31*(8), 1062–1072. https://doi.org/10.1037/pas0000732

Nichols, T.E., Holmes, A.P., 2001. Nonparametric permutation tests for functional neuroimaging: A primer with examples. *Hum. Brain Mapp. 15*(1), 1–25. https://doi.org/10.1002/hbm.1058

Nostro, A.D., Müller, V.I., Reid, A.T., Eickhoff, S.B., 2016. Correlations between personality and brain structure: A crucial role of gender. *Cereb. Cortex 7*(27), 3698–3712. https://doi.org/10.1093/cercor/bhw191

Patton, J.H., Stanford, M.S., Barratt, E.S., 1995. Factor structure of the Barratt Impulsiveness Scale. *J. Clin. Psychol. 51*(6), 768–774. https://doi.org/10.1002/1097-4679(199511)51:6%3C768::aid-jclp2270510607%3E3.0.co;2-1

Paquola, C., Vos De Wael, R., Wagstyl, K., Bethlehem, R.A.I., Hong, S.-J., Seidlitz, J., … Bernhardt, B.C., 2019. Microstructural and functional gradients are increasingly dissociated in transmodal cortices. *PLOS Biol. 17*(5), e3000284. https://doi.org/10.1371/journal.pbio.3000284

Paquola, C., Royer, J., Lewis, L.B., Lepage, C., Glatard, T., Wagstyl, K., …, Bernhardt, B., 2021. The BigBrainWarp toolbox for integration of BigBrain 3D histology with multimodal neuroimaging. *eLife 10,* e70119. https://doi.org/10.7554/eLife.70119

Poeppl, T.B., Donges, M.R., Mokros, A., Rupprecht, R., Fox, P.T., Laird, A.R., … Eickhoff, S.B., 2019. A view behind the mask of sanity: Meta-analysis of aberrant brain activity in psychopaths. *Mol. Psychiatry 24*(3), 463–470. https://doi.org/10.1038/s41380-018-0122-5

Pera-Guardiola, V., Contreras-Rodríguez, O., Batalla, I., Kosson, D., Menchón, J.M., Pifarré, J., Bosque, J., … Soriano-Mas, C., 2016. Brain structural correlates of emotion recognition in psychopaths. *PLoS ONE 11*(5), e0149807. https://doi.org/10.1371/journal.pone.0149807

Pietrini, P., Guazzelli, M., Basso, G., Jaffe, K., Grafman, J., 2000. Neural correlates of imaginal aggressive behavior assessed by positron emission tomography in healthy subjects. *Am. J. Psychiatry 157*(11), 1772–1781. https://doi.org/10.1176/appi.ajp.157.11.1772

Preckel, K., Kanske, P., Singer, T., 2018. On the interaction of social affect and cognition: Empathy, compassion and theory of mind. *Curr. Opin. Behav. Sci. 19,* 1–6. https://doi.org/10.1016/j.cobehA2017.07.010

Radecki, M.A., Cox, S.R., MacPherson, S.E., 2019. Theory of mind and psychosocial characteristics in older men. *Psychol. Aging 34*(1), 145–151. https://doi.org/10.1037/pag0000324

Rimol, L.M., Nesvåg, R., Hagler, D.J., Bergmann, Ø., Fennema-Notestine, C., Hartberg, C.B., … Dale, A.M., 2012. Cortical volume, surface area, and thickness in schizophrenia and bipolar disorder. *Biol. Psychiatry 71*(6), 552–560. https://doi.org/10.1016/j.biopsych.2011.11.026

Rogers, J.C., De Brito, S.A., 2016. Cortical and subcortical gray matter volume in youths with conduct problems: A meta-analysis. *JAMA Psychiatry 73*(1), 64–72. https://doi.org/10.1001/jamapsychiatry.2015.2423

Ronconi, L., Vitale, A., Federici, A., Pini, E., Molteni, M., Casartelli, L., 2020. Altered neural oscillations and connectivity in the beta band underlie detail-oriented visual processing in autism. *NeuroImage: Clin.* 28, 102484. https://doi.org/10.1016/j.nicl.2020.102484

Rubinov, M., Sporns, O., 2010. Complex network measures of brain connectivity: Uses and interpretations. *NeuroImage 52*(3), 1059–1069. https://doi.org/10.1016/j.neuroimage.2009.10.003

Sajous-Turner, A., Anderson, N.E., Widdows, M., Nyalakanti, P., Harenski, K., Harenski, C., … Kiehl, K.A., 2020. Aberrant brain gray matter in murderers. *Brain Imaging Behav. 14*(5), 2050–2061. https://doi.org/10.1007/s11682-019-00155-y

Sanz-García, A., Gesteira, C., Sanz, J., Paz García-Vera, M., 2021. Prevalence of psychopathy in the general adult population: A systematic review and meta-analysis. *Front. Psychol. 12,* 661044. https://doi.org/10.3389/fpsyg.2021.661044

Schurz, M., Aichhorn, M., Martin, A., Perner, J., 2013. Common brain areas engaged in false belief reasoning and visual perspective taking: A meta-analysis of functional brain imaging studies. *Front. Hum. Neurosci. 7,* 712. https://doi.org/10.3389/fnhum.2013.00712

Schurz, M., Radua, J., Aichhorn, M., Richlan, F., Perner, J., 2014. Fractionating theory of mind: A meta-analysis of functional brain imaging studies. *Neurosci. Biobehav. Rev. 42,* 9–34. https://doi.org/10.1016/j.neubiorev.2014.01.009

Schurz, M., Radua, J., Tholen, M.G., Maliske, L., Margulies, D.S., Mars, R.B., … Kanske, P., 2021. Toward a hierarchical model of social cognition: A neuroimaging meta-analysis and

integrative review of empathy and theory of mind. *Psychol. Bull. 147*(3), 293–327. http://doi.org/10.1037/bul0000303

Singer, T., Klimecki, O.M., 2014. Empathy and compassion. *Curr. Biol. 24*(18), R875–R878. https://doi.org/10.1016/j.cub.2014.06.054

Sperduti, M., Delaveau, P., Fossati, P., Nadel, J., 2011. Different brain regions related to self- and external-agency attribution: A brief review and meta-analysis. *Brain Struct. Funct. 216*(2), 151–157. https://doi.org/10.1007/s00429-010-0298-1

Spreng, R.N., Mar, R.A., Kim, A.S.N., 2009. The common neural basis of autobiographical memory, prospection, navigation, theory of mind, and the default mode: A quantitative meta-analysis. *J. Cogn. Neurosci. 21*(3), 489–510. https://doi.org/10.1162/jocn.2008.21029

Steele, V.R., Rao, V., Calhoun, V.D., Kiehl, K.A., 2017. Machine learning of structural magnetic resonance imaging predicts psychopathic traits in adolescent offenders. *NeuroImage 145,* 265–273. https://doi.org/10.1016/j.NeuroImage.2015.12.013

Timmers, I., Park, A.L., Fischer, M.D., Kronman, C.A., Heathcote, L.C., Hernandez, J.M., Simons, L.E., 2018. Is empathy for pain unique in its neural correlates? A meta-analysis of neuroimaging studies of empathy. *Front. Behav. Neurosci. 12*, 289. https://doi.org/10.3389/fnbeh.2018.00289

Toro, R., Perron, M., Pike, B., Richer, L., Veillette, S., Pausova, Z., & Paus, T. (2008). Brain size and folding of the human cerebral cortex. *Cereb. Cortex 18*(10), 2352–2357. https://doi.org/10.1093/cercor/bhm261

Tully, J., Cross, B., Gerrie, B., Griem, J., Blackwood, N., Blair, R. J., McCutcheon, R. A., 2023. A systematic review and meta-analysis of brain volume abnormalities in disruptive behaviour disorders, antisocial personality disorder and psychopathy. *Nat. Mental Health 1*, 163–173. https://doi.org/10.1038/s44220-023-00032-0

Vachon, D.D., Lynam, D.R., Johnson, J.A., 2014. The (non)relation between empathy and aggression: Surprising results from a meta-analysis. *Psychol. Bull. 140*(3), 751–773. https://doi.org/10.1037/a0035236

Valk, S.L., Bernhardt, B.C., Böckler, A., Trautwein, F.-M., Kanske, P., Singer, T., 2017. Socio-cognitive phenotypes differentially modulate large-scale structural covariance networks. *Cereb. Cortex* 27(2), 1358–1368. https://doi.org/10.1093/cercor/bhv319

van Langen, M.A.M., Wissink, I.B., van Vugt, E.S., Van der Stouwe, T., Stams, G.J.J.M., 2014. The relation between empathy and offending: A meta-analysis. *Aggress. Violent Behav. 19*(2), 179–189. https://doi.org/10.1016/j.avb.2014.02.003

Van Overwalle, F., 2009. Social cognition and the brain: A meta-analysis. *Hum. Brain Mapp. 30*(3), 829–858. https://doi.org/10.1002/hbm.20547

Van Overwalle, F., Baetens, K., 2009. Understanding others' actions and goals by mirror and mentalizing systems: A meta-analysis. *NeuroImage 48*(3), 564–584. https://doi.org/10.1016/j.NeuroImage.2009.06.009

van Veluw, S.J., Chance, S.A., 2014. Differentiating between self and others: An ALE meta-analysis of fMRI studies of self-recognition and theory of mind. *Brain Imaging Behav. 8*(1), 24–38. https://doi.org/10.1007/s11682-013-9266-8

Wechsler, D., 1997. *Wechsler Adult Intelligence Scale, third ed.* Psychological Corporation, San Antonio.

Wilson, K., Juodis, M., Porter, S., 2011. Fear and loathing in psychopaths: A meta-analytic investigation of the facial affect recognition deficit. *Crim. Justice Behav. 38*(7), 659–668. https://doi.org/10.1177/0093854811404120

Xiong, R.C., Fu, X., Wu, L.Z., Zhang, C.H., Wu, H.X., Shi, Y., Wu, W., 2019. Brain pathways of pain empathy activated by pained facial expressions: A meta-analysis of fMRI using the activation likelihood estimation method. *Neural Regen. Res. 14*(1), 172–178. https://doi.org/10.4103/1673-5374.243722

Yang, Y., Raine, A., 2009. Prefrontal structural and functional brain imaging findings in antisocial, violent, and psychopathic individuals: A meta-analysis. *Psychiatry Res. Neuroimaging 174*(2), 81–88. https://doi.org/10.1016/j.pscychresns.2009.03.012

Yang, Y., Raine, A., Joshi, A.A., Joshi, S., Chang, Y.-T., Schug, R.A., … Narr, K.L., 2012. Frontal information flow and connectivity in psychopathy. *Br. J. Psychiatry 201*(05), 408–409. https://doi.org/10.1192/bjp.bp.111.107128

Yarkoni, T., Poldrack, R. A., Nichols, T. E., Van Essen, D. C., & Wager, T. D. (2011). Large-scale automated synthesis of human functional neuroimaging data. *Nat. Methods, 8*(8), 665–670. https://doi.org/10.1038/nmeth.1635

Yeo, B.T.T., Krienen, F.M., Sepulcre, J., Sabuncu, M.R., Lashkari, D., Hollinshead, M., … Buckner, R.L., 2011. The organization of the human cerebral cortex estimated by intrinsic functional connectivity. *J. Neurophysiol.* 106(3), 1125–1165. https://doi.org/10.1152/jn.00338.2011

Zaki, J., 2017. Moving beyond stereotypes of empathy. *Trends Cogn. Sci. 21*(2), 59–60. https://doi.org/10.1016/j.tics.2016.12.004